Constancy of the Quadrupolar Interaction Product in Nanocrystalline Gallium Nitride Revealed by ^{71}Ga MAS NMR Shift Distribution

Masataka Tansho [a,*], Takayuki Suehiro [b], and Tadashi Shimizu [a]

[a] *High Field NMR Group, Research Center for Advanced Measurement and Characterization, National Institute for Materials Science (NIMS), 3-13 Sakura, Tsukuba 305-0003, Japan*

[b] *Sialon Group, Research Center for Functional Materials, National Institute for Materials Science (NIMS), 1-1 Namiki, Tsukuba 305-0044, Japan*

AUTHOR INFORMATION

*** Corresponding Author**

E-mail address: tansho.masataka@nims.go.jp (M. Tansho)

ABSTRACT

The question of whether the broad ^{71,69}Ga nuclear magnetic resonance (NMR) signal of hexagonal gallium nitride (h-GaN) at 530–330 ppm is related to the Knight shift (caused by the presence of carriers in semiconductors) is the subject of intense debate. The intensity increase observed for the narrower ^{71}Ga magic angle spinning (MAS) NMR signals above 1050 °C suggests that the broader signals do not reflect the decomposition of h-GaN. Herein, we utilized ^{71}Ga multi-quantum (MQ) MAS NMR spectroscopy to reveal that the quadrupolar interaction products for the broad signal of nanocrystalline h-GaN are almost constant in the entire shift range that we investigated, equaling 1.7 ± 0.1 MHz or similar values. Since the above parameter is sensitive to the local chemical symmetry around the Ga atom, the NMR shift distribution is considered not to be related to that of the chemical environment. Consistent with the most recent reports, including those on double-resonance ^{15}N{^{71}Ga} measurements, the Knight shift may be ascribed to defects serving as shallow donors and populating the conduction band. Thus, MQMAS measurements performed using a low-field NMR instrument or by choosing half-integer quadrupole nuclei with a large quadrupole constant such as ^{69}Ga are expected to provide important information for each Knight shift value and for analyzing the nature of semiconductors other than GaN.

Taxonomy:
Add minimum of 2 AND maximum of 6 topics
Analytical Chemistry Analysis, Industrial Inorganic Chemistry, Physical Inorganic Chemistry, Nanoparticles, Inorganic Materials, Magnetochemistry

GRAPHICAL ABSTRACT

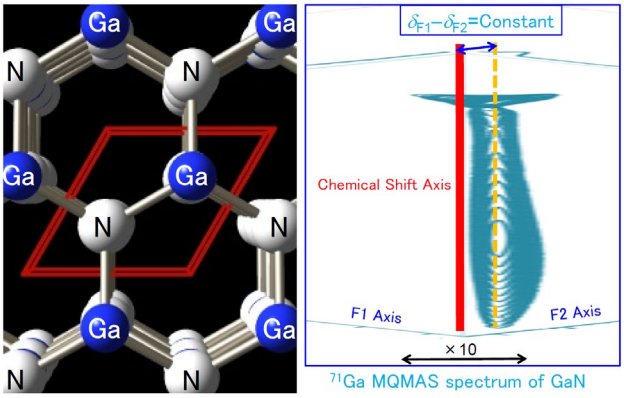

KEYWORDS: semiconductor; carrier distribution; Knight shift; MQMAS; quadrupole coupling constant; defect; Korringa rule; chemical shift axis; NMR shift.

1. Introduction

Magic-angle spinning nuclear magnetic resonance (MAS NMR) spectroscopy of inorganic solids provides valuable information on their local chemical structure. Although such structural information is typically extracted from chemical shifts, nuclear quadrupole coupling constants are similarly informative for quadrupolar nuclei with spins of $I > 1/2$, such as ^{71}Ga ($I = 3/2$) and ^{69}Ga ($I = 3/2$) [1]. In the past 30 years, gallium nitride with a hexagonal wurtzite structure (h-GaN), one of the most industrially valuable semiconductors, has been continuously investigated by NMR [2–11]. The Ga NMR signals of GaN are often known to comprise two signals: a sharp one at 330–324 ppm and a broad one at 530–330 ppm, although only one sharp ^{27}Al and one sharp ^{11}B MAS NMR signal are observed for hexagonal wurtzite–structured AlN and BN, respectively [2,12]. The sharp peaks in the above cases can be explained by a pseudo-tetrahedral MN_4 coordination (M = Ga, Al, B), which is reasonable for the hexagonal wurtzite structure. On the other hand, the broad peak can be explained by either the distribution of impurities and defects [4b–d,7,9] or that of the Knight shift related to conduction electrons (as suggested by Yesinowski et al.) [5,6,8b]. In the latter case, the shift could be related to the concentration of charge carriers in the semiconductor (n) [5,6,10,11] and is probably a function of $n^{1/3}$ [13]. Using a Korringa-type plot of the spin-lattice relaxation time (T_1) of ^{71}Ga, Yesinowski et al. [6] showed that the broad signal was mainly attributable to the Knight shift. Subsequently, Schwenzer et al. [9] showed that T_1 values experimentally determined by inversion-recovery measurements are significantly shorter than those expected in the case of the Knight-shift-only influence. They concluded that the broad shift distribution is due to nearest-neighbor inhomogeneities by ruling out large shift contributions from quadrupolar broadening using the similarity in line shape

between the ^{71}Ga NMR spectra along the F1 dimension and the F2 dimension of multi-quantum (MQ) MAS data [9]. Additionally, Yesinowski et al. [11] demonstrated that the dependence of T_1 on the saturation-recovery pulse technique implies that the true T_1 of the broad signal is not overly short compared to the simulated value. Moreover, Yesinowski et al. [14] utilized analyses including double-resonance 2D ^{15}N{^{71}Ga} measurements to reveal that ^{71}Ga, ^{14}N, and ^{15}N NMR spectra were mutually spatially correlated on a subnanometer scale, with this correlation being reasonable for the nature of the Knight shift. This evidence points toward an origin of the distribution in terms of spatially varying Knight shifts on the nanometer scale for randomly sited defects or dopants, even when the larger-scale concentration is uniform and not variable [14].

Herein, we carried out ^{71}Ga MAS NMR analysis on polycrystalline h-GaN samples prepared under a flow of ammonia [1,4a,8a,8b] under different conditions to clarify the nature of the abovementioned broad signal. The results of ^{71}Ga MQMAS NMR measurements were then compared to the typical ^{71}Ga results obtained for other gallium compounds [15,16]. Although h-GaN has previously been characterized by ^{71}Ga MQMAS (a two-dimensional NMR technique) [9], we decided to employ this powerful technique to separate isotropic and quadrupolar shifts [17] and discuss the quadrupolar interaction product (P_Q) by choosing the same ^{71}Ga nucleus.

2. Experimental

2.1. Preparation of GaN samples

Commercial GaN (Sigma-Aldrich Co., 99.99%) and Ga_2O_3 (Sigma-Aldrich Co., 99.99%) powders were used as starting materials to prepare GaN powders via two distinct synthetic routes. In route (i), commercial yellow GaN powder was heat-treated for various periods in a flowing NH_3–1.5 vol% CH_4 atmosphere at 1100 °C which produced gray powders, whereas in route (ii), GaN powders were synthesized by reduction–nitridation of Ga_2O_3 in the same atmosphere at 900 °C for various times, or at various temperatures for a constant time of 4 h [1,4a,8a]. Powders prepared via route (ii) were yellow when synthesized below 1000 °C and gray when the synthesis temperature exceeded 1000 °C. The detailed synthetic procedure has been reported in our previous work and references therein [1], and the impurity carbon content was found to be as low as 0.03 wt%. The nitrogen and oxygen contents of the as-obtained GaN samples were determined by selective hot-gas extraction (TC-436, LECO Co.). Samples prepared via route (i) using a heat treatment time of 1 h (sample A) and via route (ii) by a 5-h heating at 900 °C (sample B) were shown to have compositions of $Ga_1N_{1.000(6)}O_{0.0116(5)}$ and $Ga_1N_{0.992(6)}O_{0.069(5)}$, respectively. The phase composition and crystallite size of synthesized powders were analyzed by X-ray diffraction (XRD; SmartLab, Rigaku, 45 kV, 200 mA) using Cu $K\alpha_1$ radiation, and no crystallographic impurities were observed for samples A and B (Fig. 1). Based on the line broadening of XRD peaks, the crystallite sizes of samples A and B were 89 and 33 nm, respectively. An appreciable *a*-*b* plane orientation was observed for sample B (Figs. 1b and c) [8b].

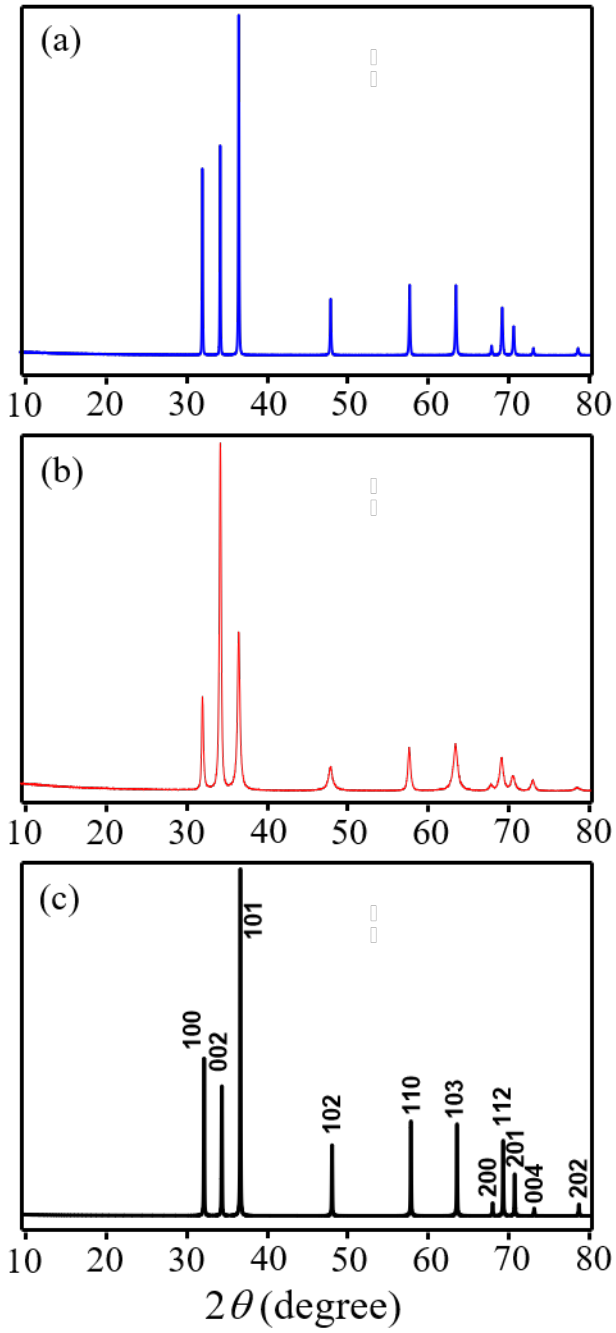

Figure 1. XRD patterns of (a) sample A, (b) sample B, and (c) simulated pattern of h-GaN (ICSD No. 54698).

2.2. Solid-state NMR

All NMR measurements were performed on a JEOL ECA 500-MHz NMR spectrometer (^{71}Ga resonance frequency = 152 MHz) using 3.2-mm double resonance MAS probes (Chemagnetics Inc.) without temperature control. All samples were spun at 20 kHz and referenced to 0 ppm utilizing 1.0 M aqueous $Ga(NO_3)_3$ as a standard. One-dimensional spectra were acquired by performing 64 scans using a 1.2-μs single-pulse sequence, which corresponded to π/2 pulses for both sharp and broad h-GaN signals (see Supporting Information). The relaxation delay was set to 20 s [6], which was sufficient for comparing the amplitudes of the above two signals. In contrast, the three-pulse (3.6, 1.3, and 15 μs) MQMAS sequence with a zero-quantum filter proposed by Amoureux et al. [18] was employed for ^{71}Ga MQMAS NMR measurements. Accumulation time was set to 1680 scans, and the relaxation delay was set to 0.5 s, which was sufficient to obtain a good signal-to-noise ratio for the broad signal in view of the shorter T_1 [6,9,11].

3. Results and discussion

Figs. 2–4 show the ^{71}Ga MAS NMR spectra of samples prepared under various reaction conditions, revealing the presence of narrow and broad signals. Specifically, narrow signals were clearly demonstrated by the pseudo-tetrahedral GaN_4 coordination that is reasonable for the

hexagonal wurtzite structure [2–9]. Moreover, the asymmetrical broadening observed for the narrow signals was larger for sample (ii) below 1050 °C.

Although only the sharp signal could be observed for sample (i) at first glance, the broad signal could also be observed upon magnification (Fig. 2(c)) [4a,8a]. Since the intensity of the broad signal did not increase with increasing heat treatment time at 1100 °C, this signal did not reflect decomposition. On the other hand, an intensity increase without sharpening was observed for the sharp signal with time, accompanied by an intensity increase of spinning sidebands. Therefore, previous studies suggest that the fraction related to the broad peak in sample (i) progressively decreased upon heat treatment in NH_3–1.5 vol% CH_4 at 1100 °C [4a,8b].

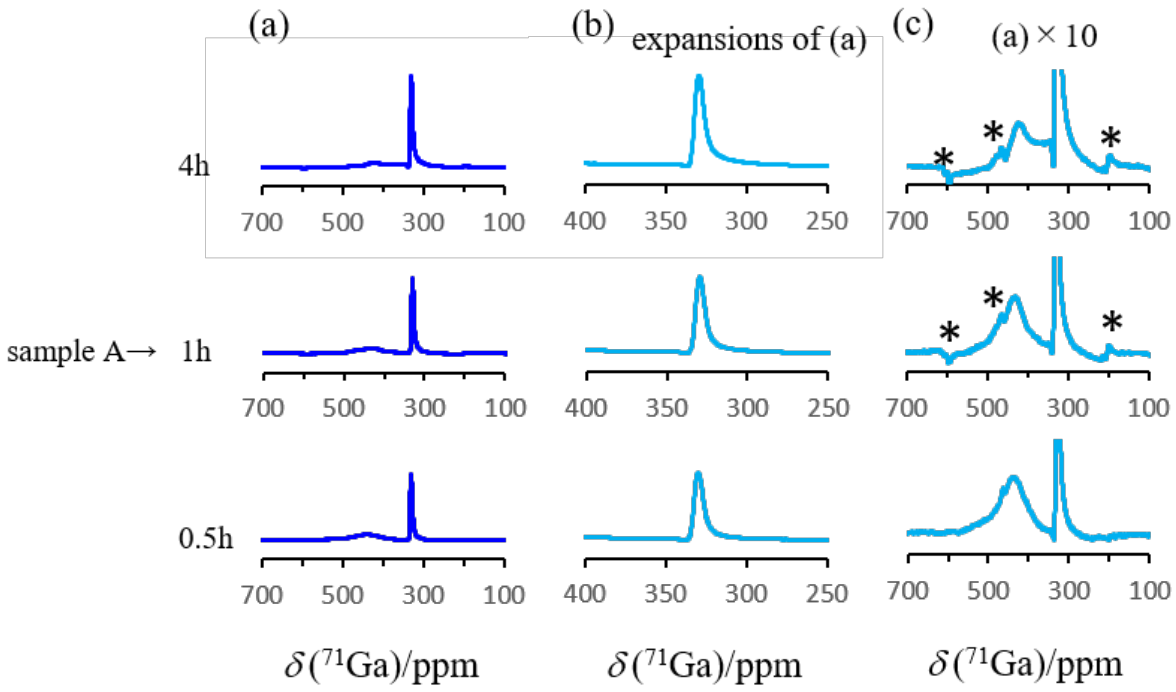

Figure 2. (a) ^{71}Ga MAS NMR spectra of samples (i) heat-treated at 1100 °C for different time periods. Spectra in (b) correspond to expansions of those in (a) in the region 400–250 ppm, and spectra in (c) correspond to expansions of those in (a) by a factor of ten, with asterisks denoting spinning sidebands.

Fig. 3 shows that the intensity of the broad signal of sample (ii) increased with increasing reaction time at 900 °C. Although the reported GaN decomposition temperatures span a wide range from below 800 °C to above 1100 °C and depend on the applied conditions and the type of GaN sample [8a], the decomposition temperature of sample (ii) was concluded to exceed 1100 °C in view of the reduction–nitridation of Ga_2O_3 in NH_3 flow [19]. Therefore, the broad signal cannot be rationalized by such decomposition but probably reflects the presence of conduction band electrons originating from the presence of oxygens as shallow electron donors at N sites, as has been suggested previously for GaN materials [14]. The increased width of the sharp signal in Fig. 3 compared to that observed in Fig. 2 was ascribed to the poor crystallinity of sample B.

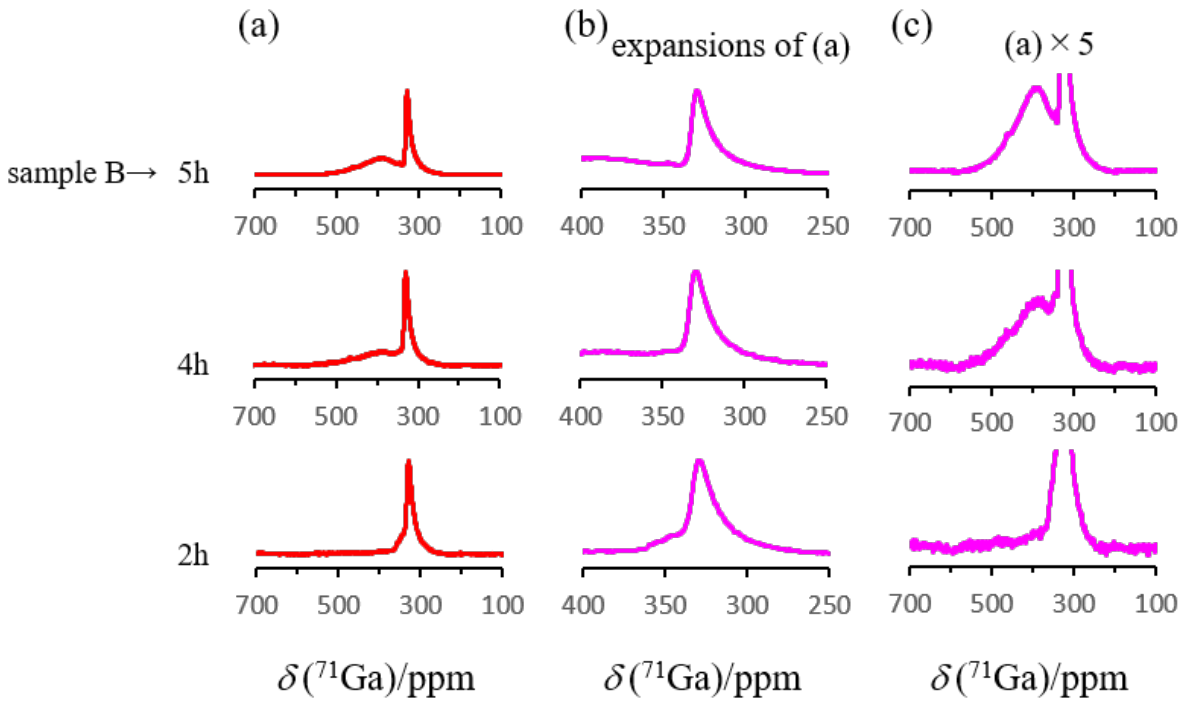

Figure 3. (a) ^{71}Ga MAS NMR spectra of samples (ii) synthesized at 900 °C for different time periods. Spectra in (b) are expansions of those in (a) from 400 to 250 ppm, and spectra in (c) are expansions of those in (a) by a factor of five.

Fig. 4 shows the ^{71}Ga MAS NMR spectra of samples (ii) synthesized under different conditions, revealing that with increasing temperature, the sharp signal of the GaN_4 structure narrowed below 1050 °C, as reported previously [4a], and became more intense above 1050 °C. On the other hand, the broad signal intensified and shifted downfield at temperatures below 1050 °C, while becoming less intense at temperatures above 1050 °C. The different behaviors observed above and below 1050 °C were in good agreement with the observed sample colors (gray and yellow, respectively). Therefore, the behavior of the sharp signal with increasing

temperature was concluded to reflect an increase in crystallinity below 1050 °C and an increase in the fraction of the sharp peak above 1050 °C [4a,8b]. The asymmetrical width of the narrow signals was thought to reflect the crystallinity distribution. On the contrary, the broad signal decrease above 1050 °C did not reflect the decomposition of GaN but rather was related to the decrease of the oxygen-rich fraction and then developed into the sharp peak by nitridation of the oxygen-rich fraction [5a,8b].

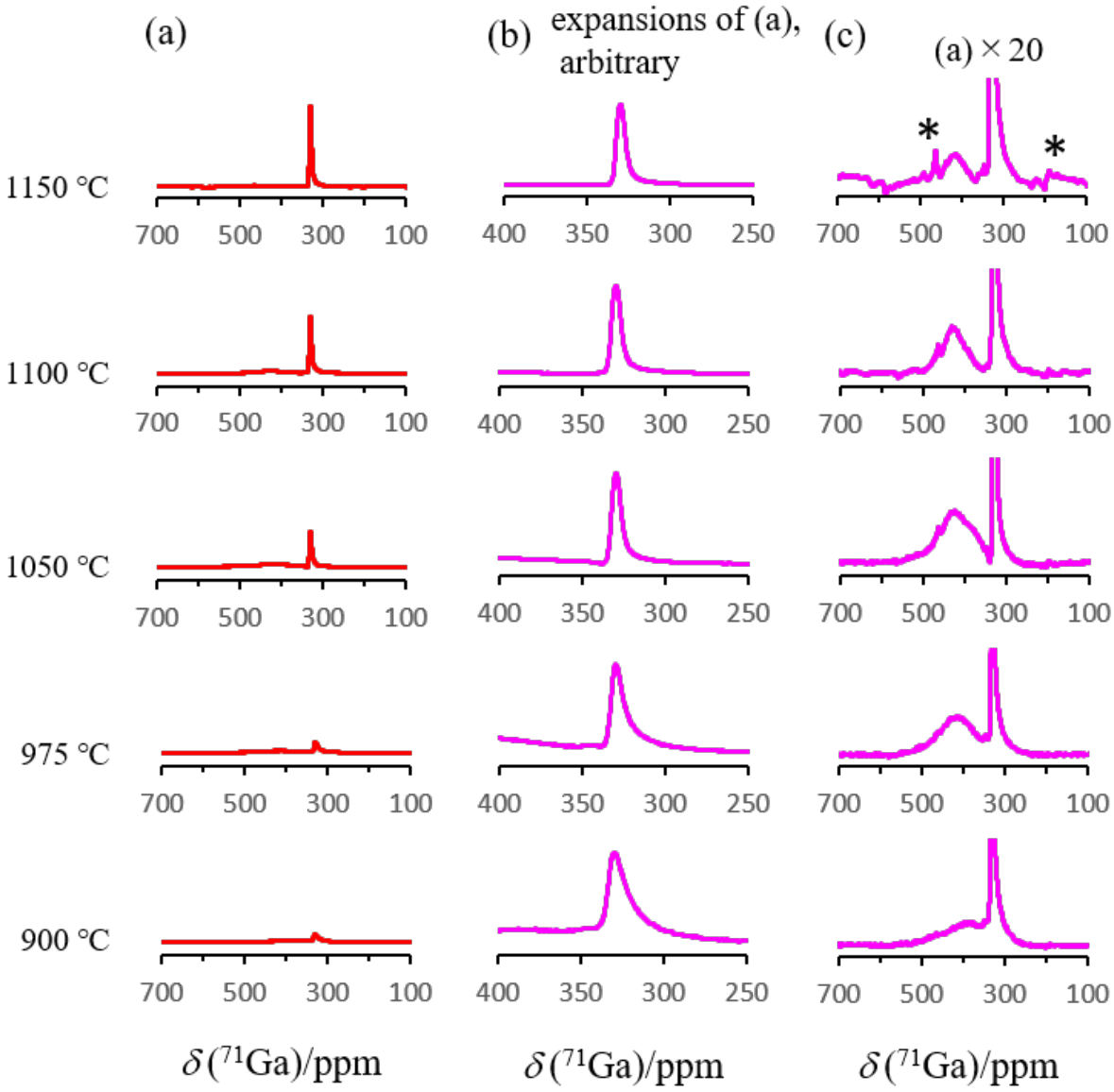

Figure 4. (a) ^{71}Ga MAS NMR spectra of samples (ii) synthesized at different temperatures for 4 h. Spectra in (b) are expansions of those in (a) from 400 to 250 ppm, and spectra in (c) are expansions of those in (a) by a factor of 20.

To understand the above behavior, samples A and B were characterized by ^{71}Ga MQMAS NMR (Fig. 5), wherein (a”) and (b”) correspond to ×10 transverse expansions of (a’) and (b’) after anti-clockwise rotation by 45° for easy viewing. For the sharp signal, the narrower widths in the F1 dimension compared to those in the F2 dimension could best be explained by the decrease in the remaining second-order quadrupolar width in the F1 dimension. Although the obtained spectra were similar to those recorded by Schwenzer et al. [9], featuring a diagonally aligned broad signal, precise analysis performed herein allowed us to extract more information.

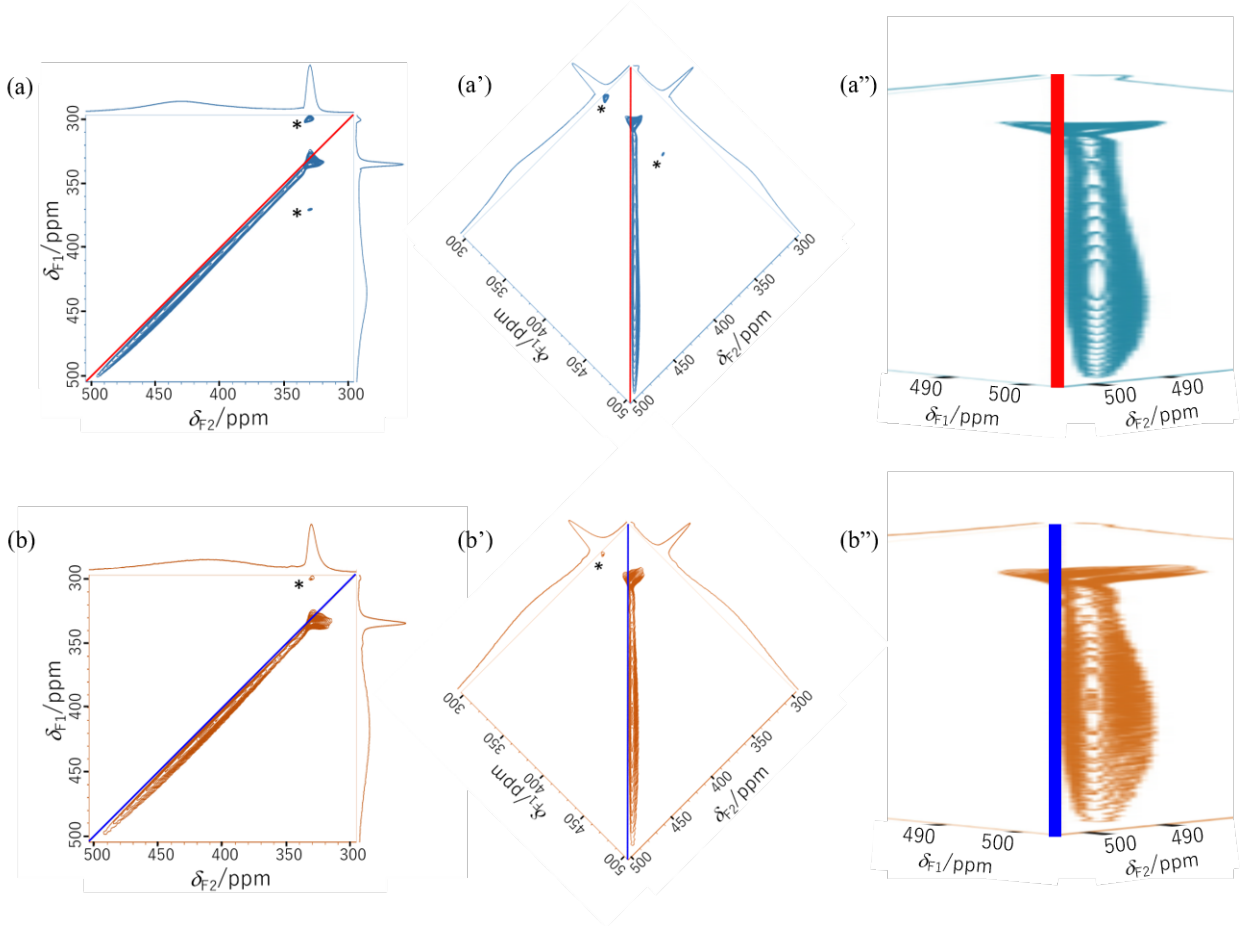

Figure 5. ^{71}Ga MQMAS NMR spectra of (a) sample A and (b) sample B, with chemical shift axes shown in red and blue, respectively, and asterisks denoting spinning sidebands. (a') and (b') are the results of anticlockwise rotation of (a) and (b) by 45°, respectively. (a'') and (b'') correspond to ×10 transverse expansions of (a') and (b'), respectively.

For simple crystalline compounds with a low extent of disorder, MQMAS signals observed after a shearing transformation are aligned parallel to the F2 axis because of the second-order quadrupolar shift, as reported for gallophosphate, GaPO-34 [15]. Since a similar alignment parallel to the F2 axis was detected for the sharp signals at 330–324 ppm, one can consider the pseudo-tetrahedral GaN_4 structures in h-GaN to result from a simple local structure with weakly pronounced chemical disorder.

However, this is not the case for the results in this study. For crystallographically disordered materials such as Ga-rich zeolites, the signals become island-shaped because of the local structure distribution [16]. For sheared three-quantum MQMAS spectra, the positions of lines in the F1 dimension are given by

$$\delta = \delta_{iso} - (10/17)\delta_{qis}, \quad (1)$$

where δ_{iso} and δ_{qis} are the isotropic chemical shift and the second-order quadrupolar shift, respectively. The positions of experimental resonances (δ_{F1} and δ_{F2}) in the F1 and F2 dimensions of the sheared MQMAS spectrum allow δ_{iso} and the quadrupolar interaction product P_Q (identical to the second-order quadrupolar effect (SOQE)) to be calculated as

$$\delta_{iso} = (17/27)\delta_{F1} + (10/27)\delta_{F2}, \quad (2)$$

$$P_Q = (680/27)^{1/2} \times 10^{-3} \times \nu_L(\delta_{F1} - \delta_{F2})^{1/2}, \quad (3)$$

where ν_L is the Larmor frequency, and P_Q is related to the quadrupole coupling constant C_Q by $P_Q = C_Q\,(1 + \eta^2/3)^{1/2}$, with the asymmetry parameter η taking values between 0 and 1 [17].

Since the diagonally aligned broad signals are almost parallel to the chemical shift axis at small δ_{qis} values, the NMR shift distributions of the broad signal are related not to the quadrupolar shift but to the isotropic shift. To clarify this situation, δ_{F2}, δ_{F1}–δ_{F2}, and P_Q for selected δ_{F1} values are listed in Tables 1 and 2.

Table 1. δ_{F2}, δ_{F1}–δ_{F2}, and P_Q values for selected δ_{F1} values of the broad signal of sample A.

δ_{F1}/ppm	δ_{F2}/ppm	δ_{F1}–δ_{F2}/ppm	P_Q/MHz
500.0	495.0 ± 0.5	5.0 ± 0.5	1.7 ± 0.1
450.0	445.0 ± 0.5	5.0 ± 0.5	1.7 ± 0.1
400.0	395.0 ± 0.5	5.0 ± 0.5	1.7 ± 0.1
350.0	345.0 ± 0.5	5.0 ± 0.5	1.7 ± 0.1

Table 2. δ_{F2}, δ_{F1}–δ_{F2}, and P_Q values for selected δ_{F1} values of the broad signal of sample B.

δ_{F1}/ppm	δ_{F2}/ppm	$\delta_{F1}-\delta_{F2}$/ppm	P_Q/MHz
500.0	495.0 ± 0.5	5.0 ± 0.5	1.7 ± 0.1
450.0	445.0 ± 0.5	5.0 ± 0.5	1.7 ± 0.1
400.0	395.0 ± 0.5	4.5 ± 0.5	1.6 ± 0.1
350.0	345.0 ± 0.5	4.0 ± 0.5	1.5 ± 0.1

As a result, for all δ_{F1} values, the same P_Q of 1.7 MHz and nearly same P_Q of 1.7–1.5 MHz with distributions of ± 0.1 MHz were observed in the ^{71}Ga spectra of h-GaN for sample A and sample B, respectively, whereas for GaO_4 coordination, P_Q or C_Q varied between 1.2 and 11 MHz, depending on the local structure [15,16,20]. Therefore, the local structural disorder represented by the broad line must be negligible for sample A and very small for sample B in the whole range of 500–350 ppm. Here, it should be noted that the "chemical shift axis" is related not only to the chemical shift distribution but also to the distribution of all other isotropic NMR shifts.

Moreover, assuming $\eta = 0$ for the axially symmetric structure of the pseudo-tetrahedral GaN_4 coordination in h-GaN for sample A, all values of $C_{Q,\,broad}$ for shifts of 500–350 ppm become identical to $P_Q = 1.7 \pm 0.1$ MHz and equal the $C_{Q,\,narrow}$ values of 1.72–1.76 MHz reported for the sharp signal in the range of 330–324 ppm [3]. This coincidence implies that the local structure of the broad signal must be identical to that of the sharp one. The above finding can also be

explained by nutation experiments considering the identical π/2 pulse lengths of both signals (see Supporting Information). The obtained $C_{Q,\,broad}$ values are difficult to rationalize assuming that the nature of the broad shift reflects the structural distribution. However, the NMR shift distribution maintaining the same C_Q is easily understood if the nature of the broader NMR shift reflects the distribution of the Knight shift, since this distribution is affected by the distribution of carriers. It is worth noting that defects are not directly correlated to the broad NMR signal via the chemical shift, although they can be related to it via the Knight shift. Oxygen shallow donors [5a,8b,14], or whatever shallow donors are responsible for Knight shifts in sample B, might produce more of a field gradient than whatever shallow donors exist in sample A.

4. Conclusion

The broad lines in the F1 axis of the MQMAS spectra were thought to reflect chemical shift distribution, and the quadrupolar interaction was concluded to be negligible at first glance [9]. However, the NMR shift distribution of the broad ^{71}Ga MAS NMR signal of h-GaN was almost unrelated to the chemical shift but was rather related to the Knight shift [5,6,8b], which, in turn, reflected the presence of defects acting as shallow donors that populate the existing conduction band with electrons. This conclusion was drawn based on the constant P_Q value of 1.7 ± 0.1 MHz or the almost constant P_Q value of 1.7–1.5 ± 0.1 MHz observed in the range of 500–350 ppm, as revealed by ^{71}Ga MQMAS measurements. Assuming the asymmetry parameter η to equal zero for axially symmetric GaN_4 coordination, the $C_{Q,\,broad}$ of sample A becomes identical to P_Q and equals the well-known $C_{Q,\,narrow}$ value of 1.72–1.76 MHz of h-GaN [3]. Hence, our

study supports the conclusion drawn by Yesinowski et al. [14] that NMR analysis reveals electronic disorders in the form of broad distributions (Knight shifts) of local metallic properties, which are shown to be spatially correlated on the subnanometer scale. The conclusion that quadrupolar parameters can be obtained for each Knight shift value is interesting and broadly relevant to conducting and degenerately doped semiconductor materials beyond GaN that manifest Knight shifts and often contain quadrupolar half-integer spin nuclei.

ASSOCIATED CONTENT

Supporting Information

The following files are available free of charge: nutation experiment details (PDF)

AUTHOR INFORMATION

Corresponding Author

*E-mail: tansho.masataka@nims.go.jp

ORCID

Masataka Tansho: 0000-0001-7986-3199

Notes

The authors declare no competing financial interests.

ACKNOWLEDGMENT

We express our gratitude to Mr. K. Deguchi and Mr. S. Ohki for their help with NMR measurements and thank Mr. Y. Yajima of NIMS for his assistance with chemical analyses.

REFERENCES

[1] Suehiro, T; Tansho, M; Shimizu, T. Quaternary Wurtzitic Nitrides in the System $ZnGeN_2$–GaN: Powder Synthesis, Characterization, and Potentiality as a Photocatalyst. *J. Phys. Chem. C* **2017**, *121*, 27590–27596.

[2] Han, O. H.; Timken, H. K. C.; Oldfield, E. Solid-State ‘‘Magic-Angle’’ Sample-Spinning Nuclear Magnetic Resonance Spectroscopic Study of Group III–V (13–15) Semiconductors. *J. Chem. Phys.* **1988**, *89*, 6046−6052.

[3] (a) Park, I.-W.; Choi, H.; Kim, H. J.; Shin, H. W.; Park, S. S.; Choh, S. H. ^{69}Ga and ^{71}Ga NMR Studies of Quadrupole Interaction in the Free-Standing GaN Single Crystals Grown by Hydride Vapor-Phase Epitaxy. *Phys. Rev. B* **2002**, *65*, 195210. (b) Corti, M.; Gabetta, A.; Fanciulli, M.; Svane, A.; Christensen, N. E. ^{69,71}Ga NMR Spectra and Relaxation in Wurtzite GaN. *Phys. Rev. B* **2003**, *67*, 064416. (c) Yesinowski, J. P.; Purdy, A. P. Defect Dynamics Observed by NMR of Quadrupolar Nuclei in Gallium Nitride. *J. Am. Chem. Soc.* **2004**, *126*, 9166−9167.

[4] (a) Jung, W.-S. Reaction Intermediate(s) in the Conversion of β-Gallium Oxide to Gallium Nitride under a Flow of Ammonia. *Mater. Lett*. **2002**, *57*, 110−114. (b) Jung, W.-S.; Park, C.; Han, S. Probing the Nitrogen Deficiency in Gallium Nitride by ^{71}Ga Magic-Angle Spinning NMR Spectroscopy. *Bull. Korean Chem. Soc.* **2003**, *24*, 1011−1013. (c) Schwenzer, B.; Hu, J.; Seshadri, R.; Keller, S.; DenBaars, S. P.; Mishra, U. K. Gallium Nitride Powders from Ammonolysis: Influence of Reaction Parameters on Structure and Properties. *Chem. Mater.* **2004**, *16*, 5088−5095. (d) Jung, W.-S.; Ra, C. S.;

Min, B.-K. Synthesis and Characterization of Gallium Nitride Powders and Nanowires Using $Ga(S_2CNR_2)_3$ (R = CH_3, C_2H_5) Complexes as New Precursors. *Bull. Korean Chem. Soc.* **2005**, *26*, 131−135.

[5] (a) Yesinowski, J. P. ^{69,71}Ga and ^{14}N high-field NMR of Gallium Nitride Films. *Phys. Status Solidi C* **2005**, *2*, 2399−2402. (b) Purdy, A. P.; Yesinowski, J. P.; Hanbicki, A. T. Synthesis, Solid-State NMR, and Magnetic Characterization of h-GaN Containing Magnetic Ions. *Phys. Status Solidi C* **2005**, *2*, 2437−2440.

[6] Yesinowski, J. P.; Purdy, A. P.; Wu, H.; Spencer, M. G.; Hunting, J.; DiSalvo, F. J. Distributions of Conduction Electrons as Manifested in MAS NMR of Gallium Nitride. *J. Am. Chem. Soc.* **2006**, *128*, 4952−4953.

[7] Schwenzer, B.; Hu, J.; Wu, Y.; Mishra, U. K. Elucidation of the Correlation between Atomic-Level Defects in GaN Nanoparticles and Photoluminescence Properties by NMR, XRD and TEM. *Solid State Sci.* **2006**, *8*, 1193−1201.

[8] (a) Drygas, M.; Olejniczak, Z.; Grzanka, E.; Bucko, M. M.; Paine, R. T.; Janik, J. F. Probing the Structural/Electronic Diversity and Thermal Stability of Various Nanocrystalline Powders of Gallium Nitride GaN. *Chem. Mater*. **2008**, *20*, 6816−6828. (b) Drygas, M.; Bucko, M. M.; Olejniczak, Z.; Grzegory, I.; Janik, J. F. High Temperature Chemical and Physical Changes of the HVPE-Prepared GaN Semiconductor *Mater. Chem. Phys.* **2010**, *122*, 537–543. (c) Jung, W.-S. Synthesis and Characterization of GaN Powder by the Cyanonitridation of Gallium Oxide Powder. *Ceram. Int.* **2012**, *38*, 5741−5756.

[9] Schwenzer, B.; Hu, J.; Morse D. E. Correlated Compositions, Structures, and Photoluminescence Properties of Gallium Nitride Nanoparticles. *Adv. Mater.* **2011**, *23*, 2278−2283.

[10] Yesinowski, J. P. Solid-State NMR of Inorganic Semiconductors. *Top. Curr. Chem.* **2012**, *306*, 229−312.

[11] Yesinowski, J. P. Finding the True Spin-Lattice Relaxation Time for Half-Integral Nuclei with Non-Zero Quadrupole Couplings. *J. Magn. Reson*. **2015**, *252*, 135−144.

[12] Tansho, M.; Komatsu, S.; Shimizu, Y.; Moriyoshi Y. ^{11}B and ^{10}B MAS NMR Studies of Distorted Tetrahedral Coordination of Wurtzite Boron Nitride. *Diamond Relat. Mater.* **2003**,*12*,1169–1172

[13] Wolf, D. *Spin-Temperature and Nuclear-Spin Relaxation in Matter*; Clarendon Press: Oxford, 1979; Chapter 15.

[14] Yesinowski, J. P.; Berkson, Z. J.; Cadars, S.; Purdy, A. P.; Chmelka, B. F. Spatially Correlated Distributions of Local Metallic Properties in Bulk and Nanocrystalline GaN. *Phys. Rev. B* **2017**, *95*, 235201.

[15] Amri, M.; Ashbrook, S. E.; Dawson, D. M.; Griffin, J. M.; Walton, R. I.; Wimperis, S. A Multinuclear Solid-State NMR Study of Templated and Calcined Chabazite-Type GaPO-34. *J. Phys. Chem. C* **2012**, *116*, 15048−15057.

[16] Arnold, A.; Steuernagel, S.; Hunger, M.; Weitkamp J. Insight into the Dry-Gel Synthesis of Gallium-Rich Zeolite [Ga]Beta. *Microporous Mesoporous Mater.* **2003**, *62*, 97−106.

[17] Engelhardt, G.; Kentgens, A. P. M.; Koller, H.; Samoson, A. Strategies for Extracting NMR Parameters from ^{23}Na MAS, DOR and MQMAS Spectra. A Case Study for $Na_4P_2O_7$. *Solid State Nucl. Magn. Reson.* **1999**, *15*, 171−180.

[18] Amoureux, J. P.; Fernandez, C.; Steuernagel, S. Z Filtering in MQMAS NMR. *J. Magn. Reson*. *A* **1996**, *123*, 116−118.

[19] (a) Xiao, H. D.; Ma, H. L.; Lin,Z. J.; Ma, J.; Zong, F. J.; Zhang, X. J. Thermal Stability of GaN Powders in the Flowing Stream of N_2 Gas. *Mat. Chem. Phys.* **2007**, *106*, 5–7. (b) Kiyono, H.; Sakai, T.; Takahashi, M.; Shimada S. Thermogravimetric Analysis

and Microstructural Observations on the Formation of GaN from the Reaction between Ga_2O_3 and NH_3. *J. Cryst. Growth* **2010**, *312*, 2823−2827.

[20] (a) Timken, H. K. C.; Oldfield, E. Solid-state Gallium-69 and Gallium-71 Nuclear Magnetic Resonance Spectroscopic Studies of Gallium Analogue Zeolites and Related Systems. *J. Am. Chem. Soc*. **1987**, *109*, 7669–1673. (b) Massiot, D.; Farnan, I.; Gautier, N.; Trumeau, D.; Trokiner, A.; Coutures, J. P. ^{71}Ga and ^{69}Ga Nuclear Magnetic Resonance Study of β-Ga_2O_3: Resolution of Four- and Six-fold Coordinated Ga Sites in Static Conditions. *Solid State Nucl. Magn. Reson.* **1995**, *4*, 241–248. (c) Ash, J. T.; Grandinetti, P. J. Solid-state NMR Characterization of ^{69}Ga and ^{71}Ga in Crystalline Solids. *Magn. Reson. Chem*. **2006**, *44*, 823–831.